ECOGRAPHY

Research article

Integrated species distribution models fitted in INLA are sensitive to mesh parameterisation

Lea I. Dambly[1,2], Nick J. B. Isaac[1], Kate E. Jones[2,3], Katherine L. Boughey[4] and Robert B. O'Hara[5]

[1]UK Centre for Ecology and Hydrology, Wallingford, UK
[2]Dept of Genetics, Evolution and Environment, Centre for Biodiversity and Environment Research, Univ. College London, London, UK
[3]Inst. of Zoology, Zoological Society of London, London, UK
[4]Bat Conservation Trust, London, UK
[5]Dept of Mathematical Sciences, Norwegian Univ. of Science and Technology, Trondheim, Norway

Correspondence: Lea I. Dambly (lea.dambly@natcapresearch.com)

Ecography
2023: e06391
doi: 10.1111/ecog.06391
Subject Editor: Thorsten Wiegand
Editor-in-Chief: Miguel Araújo
Accepted 1 March 2023

The ever-growing popularity of citizen science, as well as recent technological and digital developments, have allowed the collection of data on species' distributions at an extraordinary rate. In order to take advantage of these data, information of varying quantity and quality needs to be integrated. Point process models have been proposed as an elegant way to achieve this for estimates of species distributions. These models can be fitted efficiently using Bayesian methods based on integrated nested Laplace approximations (INLA) with stochastic partial differential equations (SPDEs). This approach uses an efficient way to model spatial autocorrelation using a Gaussian random field and a triangular mesh over the spatial domain. The mesh is constructed by user-defined variables, so effectively represents a free parameter in the model. However, there is a lack of understanding about how to set these mesh parameters, and their effect on model performance. Here, we assess how mesh parameters affect predictions and model fit to estimate the distribution of the serotine bat, *Eptesicus serotinus*, in Great Britain. A Bayesian INLA model was fitted using five meshes of varying densities to a dataset comprising both structured observations from a national monitoring programme and opportunistic records. We demonstrate that mesh density impacted spatial predictions with a general loss of accuracy with increasing mesh coarseness. However, we also show that the finest mesh was unable to overcome spatial biases in the data. In addition, the magnitude of the covariate effects differed markedly between meshes. This confirms that mesh parameterisation is an important and delicate process with implications for model inference. We discuss how species distribution modellers might adapt their use of INLA in the light of these findings.

Keywords: citizen science, INLA, integrated species distribution model (ISDM), point process model, statistics

NORDIC SOCIETY OIKOS

www.ecography.org

Introduction

Species distribution models (SDMs) are a commonly used tool in ecological research to model species distributions and abundances over space and time. The data available for these models have greatly increased in past years owing to the digital and technical changes in data collection (Hampton et al. 2013, Guillera-Arroita 2016). New monitoring technologies such as passive acoustic monitoring, and the continuously increasing popularity of citizen science, are just two innovations that drive this growing data availability (August et al. 2015, Bayraktarov et al. 2019, Gibb et al. 2019). However, this increase in data does not come without challenges for species distribution modelling. These data vary in their information content and their attributes, for example sampling method or spatial extent, but they all include useful information about species abundance and occurrence. Traditionally, these differences in the data meant that one dataset would be chosen for modelling, while others with potentially vital information were discarded. To take advantage of this large amount of information, it is necessary to integrate data of varying quantity and quality. Integrated distribution models (IDMs) are a recently emerging approach that allow different datasets to be used while accounting for the strengths and weaknesses of each (Fletcher et al. 2019, Miller et al. 2019, Zipkin et al. 2019, Isaac et al. 2020). One method to implement IDMs is the joint-likelihood approach (Pacifici et al. 2017). Here, IDMs are formed through submodels that combine an unobservable latent state (e.g. the true distribution of a species) with one or more observation models, which describe how data were generated from the latent state. While the observation models are unique to a dataset, the latent state and the parameters describing it are shared between all datasets through a joint likelihood (Pacifici et al. 2017).

Although the combination of different data sources for parameter estimation is not novel to ecological modelling, the innovation of IDMs lies with their ability to make use of different ecological 'currencies' (e.g. occupancy and abundance data), or data of different spatial resolutions (Isaac et al. 2020). This can be achieved by using point process models, which describe the continuous spatial distribution of points (Dorazio 2014, Renner et al. 2015, Bowler et al. 2019, Adde et al. 2021, Farr et al. 2021). The location of points is modelled with an intensity that describes the likelihood of points being present. Points in this context are individuals, meaning a high intensity implies that individuals are more likely to be present. The intensity can be estimated using a log-Gaussian Cox process (Møller et al. 1998), which can be interpreted as a latent Gaussian random field with a Matérn covariance function, a type of statistical model used for spatial processes over a continuous space. These models include a spatially structured effect which is used to account for spatial autocorrelation unexplained by covariates in the model. The fitting of these models can be troublesome and computationally expensive. However, the stochastic partial differential equation (SPDE) approach of the integrated nested Laplace approximation (INLA) method enables Bayesian inference of the Gaussian Markov random field (continuous) by approximating it with a discrete triangulated mesh (Lindgren et al. 2011, Illian et al. 2013, Lindgren and Rue 2015). This mesh divides the study area into a set of non-intersecting triangles.

Several studies have now demonstrated that IDMs are an efficient approach to combining multiple sources of data that improve estimation and can account for biases in data collection (Fithian et al. 2015, Koshkina et al. 2017, Peel et al. 2019). While IDMs can be fitted with more established Markov chain Monte Carlo (MCMC) software (Bowler et al. 2019, Chevalier et al. 2021, Gilbert et al. 2021, Strebel et al. 2022), INLA is suggested to be a more computationally efficient alternative (Isaac et al. 2020). Despite its growing popularity, INLA is still poorly understood in ecology and conservation. In particular, spatial point process methodology has been slow to be picked up, potentially due to a lack of accessible literature for the applied user community (Renner et al. 2015, Illian and Burslem 2017). As a result, discretising the study domain into grid cells remains the norm when estimating species distributions. The common issue of this approach is that a spatial scale needs to be fixed, which makes it harder to account for within-grid heterogeneity (Isaac et al. 2020). While strictly this problem does not arise when using a mesh approach, it is nonetheless an approximation of the intensity surface. The finer the mesh, the finer the approximation can be, but this comes at a higher computational cost (Blangiardo and Cameletti 2015).

Given that one of the proposed applications of IDMs is a better use of the vast amount of data generated by citizen scientists (Johnston et al. 2022), which are often used by applied researchers and conservation practitioners, it is vital to advance practical understanding of the mesh parameterisation on model inferences. The aim of our study was to test the impact of mesh density, and thus approximation, on model predictions of an IDM fitted with the INLA–SPDE approach. Specifically, we compare the statistical properties of five models that differ only in their mesh parameters. We used data from a structured citizen science monitoring programme and integrated them with opportunistic data from an ad hoc recording scheme to model the distribution of the serotine bat *Eptesicus serotinus* in Great Britain (consisting of England, Scotland, and Wales). *E. serotinus* is common at its core range in mainland Europe but is considered less common in the United Kingdom (consisting of England, Scotland, Wales, and Northern Ireland), where it is spatially restricted to southern England and Wales (Dietz and Helversen 2009). The species is protected by domestic and international legislation throughout its range, which makes accurate information about its distribution and environmental relationships important for conservation.

Material and methods

Data and covariates

We used two sources of *E. serotinus* data for our study (Fig. 1), the first from the field survey that is part of the

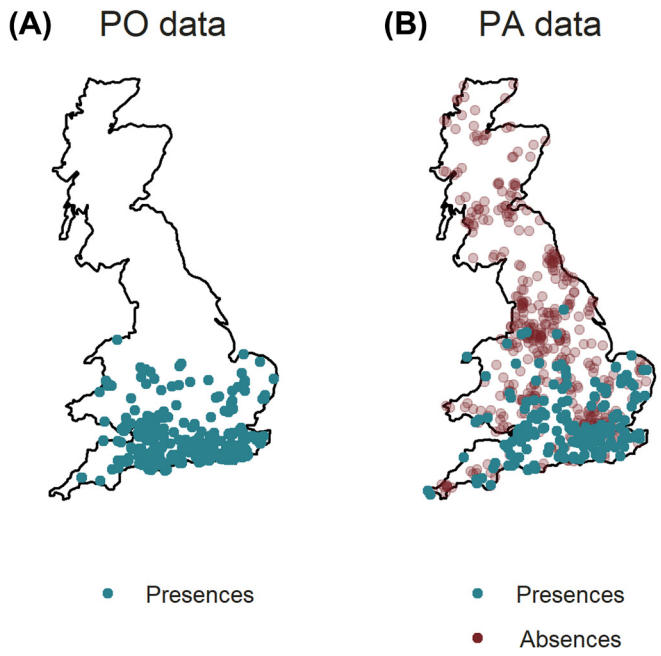

Figure 1. Spatial distribution of data modelled in the integrated species distribution models. Map A shows presences of *Eptesicus serotinus* in Great Britain from the presence-only (PO) dataset, which was sourced from the NBN Atlas (n = 1374). Map B shows presences and absences (PA) of *E. serotinus* in Great Britain from the presences and absences (PA) dataset, which was sourced from the National Bat Monitoring Programme (NBMP) field survey (n = 666).

National Bat Monitoring Programme (NBMP) of the UK's Bat Conservation Trust (BCT). The field survey consists of a structured mobile acoustic survey where trained volunteers walk an approximately 3 km long transect within a randomly allocated 1 km grid square. Counts of the number of bat passes are made at 12 points along the transect. For our study, we reduced the data to presences and absences (PA) per site (n = 666) because it is likely that the counts reflect bat activity (a combination of species abundance and time spent in the area) rather than true abundance, due to their foraging behaviour. There is a risk of recording the same bat multiple times, which would add additional uncertainty to the analysis. The second dataset was from the National Biodiversity Network (NBN) Atlas which combines presence-only (PO) data from multiple sources. We excluded data that were not verified by expert verifiers, were from the NBMP field survey, and where coordinate uncertainty was more than 1 km (remaining data n = 1374). For both datasets, data from 2005–2015 were used, which maximised the number of data points while assuming that the species' range was stable over the chosen time period. While the NBMP field survey data are collected in a spatially random way (Barlow et al. 2015), most of the data that make up the NBN dataset are not. For example, a large number of the records come from unstructured, that is spatially non-random, surveys. These are commonly uneven in their geographical distribution as recorders are more likely to record where human population density is high or where they have pre-existing knowledge about the presence of a species (Dennis and Thomas 2000, Botts et al. 2011, Geldmann et al. 2016, Mair and Ruete 2016).

We chose the following environmental covariates for analysis of the impact of mesh dimensions: mean annual temperature (°C) averaged across our study period (Robinson et al. 2017); percentage cover arable land, broadleaf woodland, and improved grassland (Rowland et al. 2017) (Fig. 2). These covariates were chosen because *E. serotinus* roosting sites are known to be associated with arable land, improved grassland (Tink et al. 2014), and broadleaf woodland (Boughey et al. 2011). Their foraging sites are generally determined by the habitat available to them around their roosting site, and they are able to exploit a large variety of habitat for foraging (Catto et al. 1996). All covariate values were scaled and centred (mean = 0, SD = 1). Empirical variograms were calculated for all four covariates to explore the spatial autocorrelation in each.

Modelling

The R code for data preparation and model fitting was based on the R-package (www.r-project.org) 'PointedSDMs' ver. 0.2.1.9004 (https://github.com/oharar/PointedSDMs), which is built on the widely used 'R-INLA' package (Lindgren and Rue 2015). It was implemented in R ver. 4.0.0 (www.r-project.org) with INLA 21 February 2023 (for INLA methodology Rue et al. 2009; for SPDE methodology Lindgren et al. 2011, Krainski 2019; for software http://www.r-inla.org).

We modelled the distribution of *E. serotinus* as a log-Gaussian Cox process whose intensity varies as a function of our environmental covariates and the spatial field. A sub-model was developed for each dataset, and these were integrated together via a joint-likelihood. The PA data were assumed to follow a Bernoulli distribution (Eq. 1):

$$Y_i \; Bernoulli\left(p_i\right), i = 1, 2, \ldots, n \tag{1}$$

$$cloglog\left(p_i\right) = \alpha_1 + \sum_{i=1}^{L} \beta_i x_{i,(s)} + f\left(s\right)$$

where the response variable Y_i (presence or absence) was modelled as the probability of presence p_i within a sampled quadrat i following a single Bernoulli trial. The log intensity was linked to p_i via a cloglog link (Kéry and Royle 2016), where α_1 is the intercept, $\sum_{i=1}^{L} \beta_i x_{i,(s)}$ the sum of the environmental covariates (mean annual temperature, percentage cover arable land, broadleaf woodland, and improved grassland) and $f\left(s\right)$ a spatial random effect. The PO data were modelled as the expected number of individuals in an area with a Poisson distribution (Eq. 2):

$$N(A) \; Poisson\left(\int_A \lambda(s) d(s)\right) \tag{2}$$

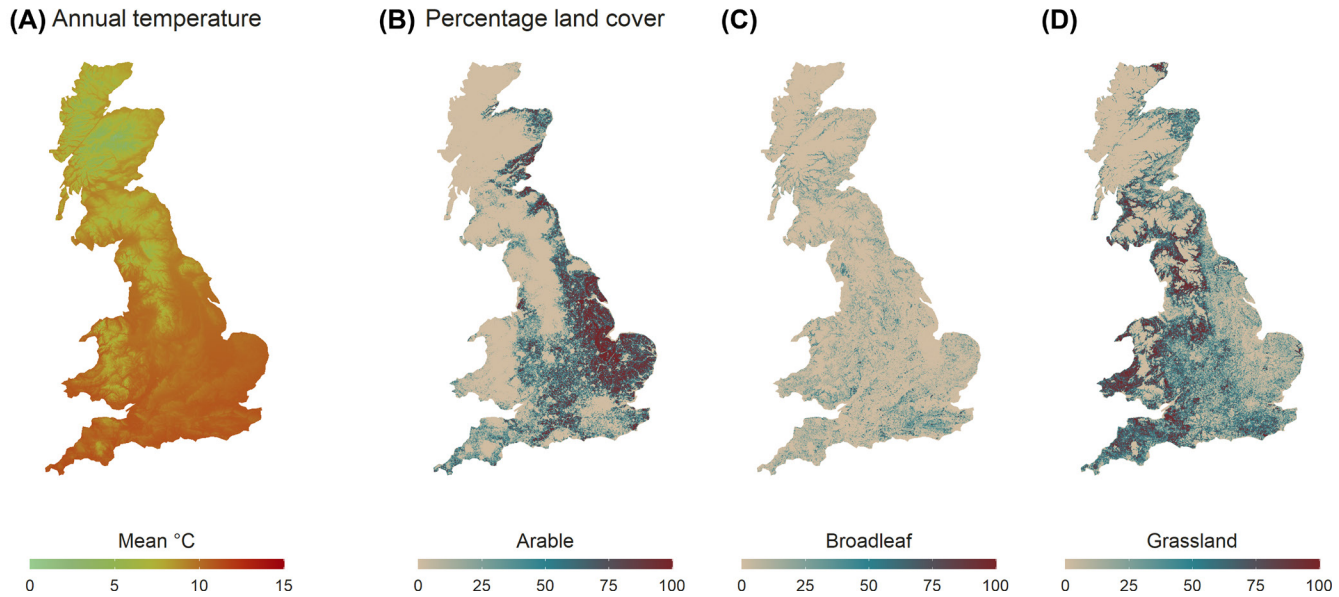

Figure 2. Maps of the environmental covariates used in the integrated species distribution models (SDMs). Map (A) shows the mean annual temperature 2005–2015 in degrees Celsius from the CHESS-met dataset (Robinson et al. 2017). Maps (B), (C), and (D) show the percentage land cover of arable, broadleaf woodland, and improved grassland from the UK Centre for Ecology & Hydrology land cover map 2015 dataset (Rowland et al. 2017). The land cover map 2015 was produced by classifying satellite images from 2014 and 2015 into different habitat classes.

$$log\left(\lambda\left(s\right)\right) = \alpha_2 + \sum_{i=1}^{L} \beta_i x_{i,(s)} + f\left(s\right)$$

where N is the expected number of presences in an area A, λ is the mean intensity function, α_2 is the intercept, and $\sum_{i=1}^{L} \beta_i x_{i,(s)}$ and $f\left(s\right)$ are the same terms as in the PA data: these model the actual distribution of *E. serotinus*. To fit the PO data as a Poisson process, we derived integration points and set weights in the likelihood following Simpson et al. (2016). We integrated our two datasets via a joint-likelihood approach, where the likelihoods of each dataset are multiplied, and some parameters, β_i and $f\left(s\right)$, are shared between the individually modelled datasets (Kéry and Royle 2016).

Mesh parameterisation

We constructed five meshes by using an outline of mainland Great Britain as a domain boundary (Fig. 3). There are two main parameters we can define which influence the density of the mesh. The units for these parameter values will depend on the input data, in our case they are in kilometres. The first parameter, which must always be specified, consists of two arguments which set the maximum allowed triangle edge length inside (*max.edge1*) and outside (*max.edge2*) of the boundary. *Max.edge1* is recommended to be set as smaller than 1/5 of the range (Bakka 2018), which is the radius around an observation at which autocorrelation falls below a threshold of 0.1. Spatial autocorrelation is driven by many different factors, which can be difficult to determine (Mielke et al. 2020). *E. serotinus* is considered a non-migratory species with seasonal flights of under 100 km (Hutterer 2005). Its mean home-range radius in the UK – that is, the mean of the greatest straight line distance an individual has been recorded from the roost in telemetry studies – is reported to be 7 km (Boughey et al. 2011). However, on rare occasions, individuals in the UK have been found to travel greater distances of over 41 km (Robinson and Stebbings 1997). While we can assume that spatial autocorrelation is related to the home range of a species, this would likely be a severe underestimate due to the various extrinsic and intrinsic drivers of spatial autocorrelation (Mielke et al. 2020). We therefore chose a value of 5 for *max.edge1* of the first model and added 20 for each subsequent model to account for a variety of reasonable range values. The value of *max.edge2* should always be larger than *max.edge1*, as the space outside the boundary only exists to avoid boundary effects and no predictions are generated there, which is why we always set *max.edge2* to 150. The second parameter (*cutoff*) is optional and refers to the shortest allowed distance between two mesh vertices. This parameter must always be smaller than *max.edge*. As per recommendations, we set *cutoff* to be 1/5 of *max.edge1* (Bakka 2017) (Table 1).

Prior specification

We used the default priors for the fixed effects, which are Gaussian with a 0 mean and a precision of 0.001. For the spatial effect, we ran models twice, once with default priors and once with penalised complexity (PC) priors, which penalise departure from a base model (Simpson et al. 2017). For the default priors, the model seeks values that are sensible for the mesh, so they differ between meshes. The PC priors are defined through probability statements about the variation

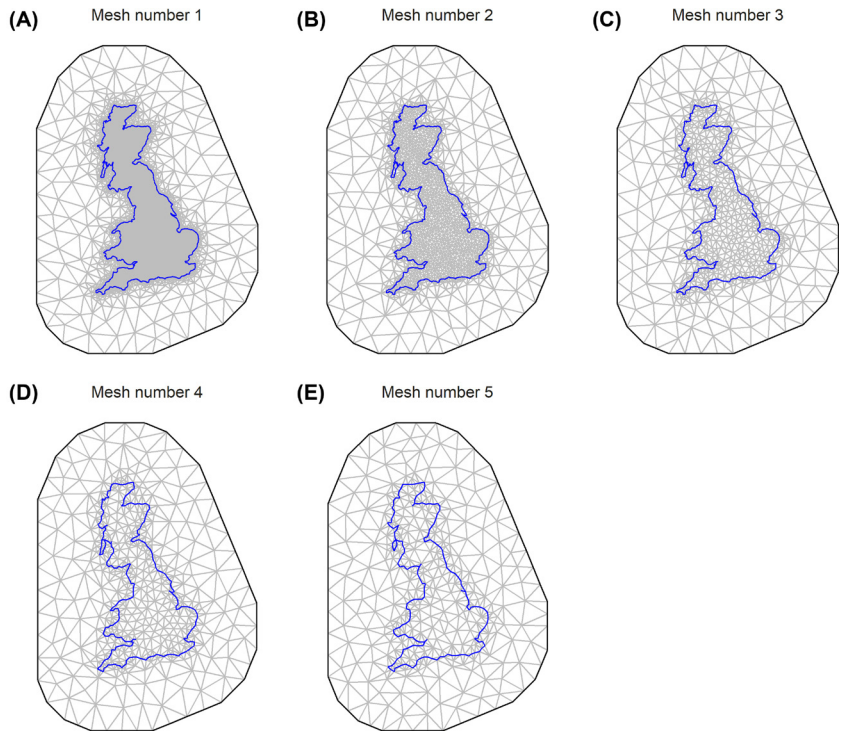

Figure 3. Maps of the five meshes from finest mesh (A – Mesh number 1) to coarsest (E – Mesh number 5). The blue outline is the mesh boundary within which distributions will be predicted. The area between the blue and black lines serves to prevent boundary effects.

in and range of the spatial effect. In theory, the PC priors are not independent from the mesh as they could be specified to contradict the mesh: e.g. if the prior range suggests a very small range but the mesh is set with a large range in mind. The prior for the SD δ is defined by $P(\delta > \delta_0) = p$, where we set $\delta_0 = 1$ and $p = 0.5$. This means that we consider an SD above 1 as likely. The prior for the range κ is defined through $P(\kappa < \kappa_0) = p$, where we set $\kappa_0 = 7$ and $p = 0.01$. This was motivated by our knowledge of the mean home-range radius of *E. serotinus* being 7 km (Boughey 2011). We assume that the range of the spatial effect – that is, the distance at which two points are independent – is very unlikely to be below 7 km.

Further model variants

Because of the posterior range estimates given by the models described above, and because we assume that spatial autocorrelation may be driven by factors operating on a much larger scale than the home range, we also ran models with two different sets of priors for the range κ, which we set as $P(\kappa < 50) = 0.01$, as well as $P(\kappa < 100) = 0.01$. The SD δ remained the same. We did not change the meshes to reflect these range values as our main goal was to investigate the effect of a wide range of potential mesh parameterisations on model results. In addition, we also ran models with a fixed range κ ($\kappa_0 = 7$) and a fixed SD δ ($\delta_0 = 1$). Finally, we also ran models (using the initial set of PC priors $P(\kappa < 7) = 0.01$ and $P(\delta > 1) = 0.5$) with an additional spatial effect for the PO dataset, to account for the additional spatial bias in these data (following Simmonds et al. 2020).

Table 1. Values of different mesh parameters used to construct the five different meshes. Mesh 1 is the finest and 5 is the coarsest. *Max. edge1* sets the maximum triangle edge length inside the boundary, while *max.edge2* sets it outside the boundary. *Cutoff* determines the shortest allowed distance between two mesh vertices.

Mesh number	max.edge1	max.edge2	cutoff
1	5	150	1
2	25	150	5
3	45	150	9
4	65	150	13
5	85	150	17

Model evaluation and comparison

To investigate the effect of mesh density on overall inference, we compared the spatial predictions of each model by mapping the mean as well as the SD of the estimated intensity on a regular grid with a 5 km resolution. Next, we focused on the individual model components, namely the spatial effect and the fixed effects. We mapped the mean and SD of the intensity as a function of the spatial effect on its own to visually assess its smoothness. It is important to note that we are using the term smoothness in a qualitative way to describe the shape of the spatial effect (Miller et al. 2020). In addition, we plotted the posterior range of the spatial effect, that is the spatial scale of the correlation, for each model. In order to measure the proportion of the mean intensity explained by the spatial effect, we calculated the correlation (R^2) between

the total mean intensity and the intensity as a function of the spatial effect. To further compare the different models, we plotted the posterior estimates of the environmental covariates, as well as the individual and shared intercepts.

For each parameter, we report the mean of the posterior distribution and 95% credible intervals. We also report the Watanabe Akaike information criterion (WAIC) for each model as a measure of goodness-of-fit, which is calculated within INLA. A smaller WAIC suggests a better model fit. For the models' predictive performance, we used the Log-score, which is a summary measure of the conditional predictive ordinate (CPO). The CPO is a cross-validation method estimating the leave-one-out predictive distribution, which is also calculated within INLA (Held et al. 2010). A higher Log-score suggests a better predictive performance. These measures allow us to compare the fit and predictive performance of models fitted with and without PC priors. However, it is not possible to use these measures to compare models fitted with different meshes as INLA evaluates the deviance and CPO at the integration points, the number of which varies between different meshes and as such would mean comparing models with different datasets.

Results

Effect of prior specification

Overall, we found that any effect of changing the priors was dwarfed by the variation between meshes, highlighted by the similarities in WAIC and CPO (Supporting information). For simplicity, here we present the results of the five models with one set of PC priors $\left(P\left(\kappa<7\right)=0.01\right)$ since this is the generally recommended practice for SPDE models. See Supporting information for results for comparable models with different prior specifications, models with default priors, models with $P\left(\kappa<50\right)=0.01$ and $P\left(\kappa<100\right)=0.01$, models with fixed PC priors, and models with an additional spatial effect for the PO dataset.

How do the spatial predictions differ between models?

The maps of the mean intensity (Fig. 4) share one overall similar trend, which is that a generally higher intensity is predicted for the south of England (see Supporting information for SD). However, the amount of land predicted to have high intensities (values above zero) noticeably increases from the finest mesh model (model with mesh number 1, Fig. 4A) to the coarsest mesh model (model with mesh number 5, Fig. 4E). Despite these broadly similar spatial trends, it is remarkable how much the finer spatial patterns vary between the models. For example, models with mesh numbers 1–3 (Fig. 4A–C) predict areas of high intensity in the Midlands, while models with mesh numbers 4 and 5 do not (Fig. 4D–E). The model with mesh number 1 in particular seems to perfectly reproduce the spatial patterns found in our observed data, which suggests that it is overfitting (Supporting information). It is also noticeable that, for all but the finest mesh model, the intensity tends to increase near the coast. This is especially visible at the Scottish peninsula Kintyre on the west coast, which is outside the known range of *E. serotinus*. These patterns may point to some issues with boundary effects, despite the large outer extension of our meshes (Fig. 3).

How does the spatial effect differ between models?

Looking at the individual model components, the spatial effect does get noticeably smoother (that is, less disjointed) with decreasing mesh density (Fig. 4) (see Supporting information for SD). This is confirmed by the posterior range of the spatial effect, which varies from approximately 30 km in the finest mesh model to around 200 km in the coarsest (Supporting information). The spatial effect of each model exhibits very similar spatial patterns to the overall predicted intensity. This is reflected by the R^2 measures, which are all close to 1 and indicate that in all models over 90% of the predictions were explained by the spatial effect (Fig. 5). There does not seem to be a directional effect related to the mesh coarseness, as the model with mesh number 1 (Fig. 5A) actually has the highest R^2, and the model with mesh number 3 the lowest (Fig. 5C).

How do the covariate effects differ between models?

The empirical semi-variograms for each covariate showed evidence for spatial autocorrelation in temperature, arable, and grassland. Semi-variance for these variables increased with increasing distance, but was comparatively stable for broadleaf (Supporting information). The comparison of the posterior estimates for the environmental covariates revealed differences in effect size and direction between the models (Fig. 6). The first pattern to emerge is that, as the mesh becomes coarser, the effect of broadleaf (Fig. 6C) and grassland (Fig. 6D) generally becomes bigger. On the other hand, temperature (Fig. 6A) and arable (Fig. 6B) show almost an inverse pattern of one another, where the effect becomes increasingly positive (temperature) or increasingly negative (arable) from the model with mesh number 1 to the model with mesh number 3; peaks (negative or positive) at the model with mesh number 3; and then gets close to zero and non-significant for the model with mesh number 5. In contrast, the effects of the intercepts of the individual datasets show little differences between the models (Supporting information). Only the effect of the intercept of the integration points (Supporting information) becomes considerably more negative with increasing mesh coarseness.

Discussion

This study set out to investigate the effect of mesh density on model performance using an IDM fitted with an

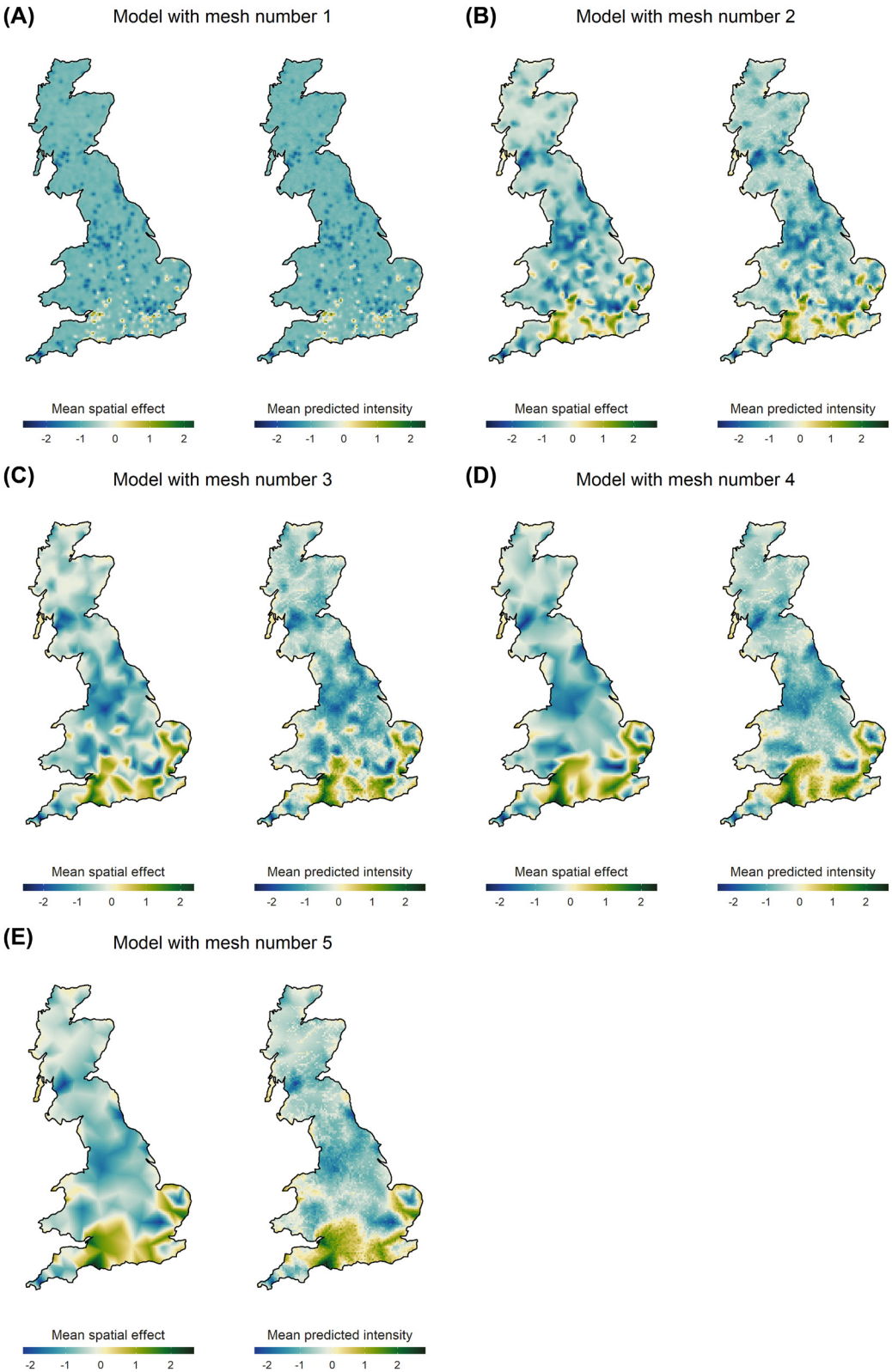

Figure 4. Maps of the mean predicted spatial effect (left) and the mean predicted intensity (right) from the integrated species distribution models (SDMs) estimated for *Eptesicus serotinus*. The maps are presented from finest to coarsest mesh (Fig. 3, Table 1), meaning map (A) shows the results from the model with mesh number 1 (the finest mesh) and map (E) shows the results from the model with mesh number 5 (the coarsest mesh).

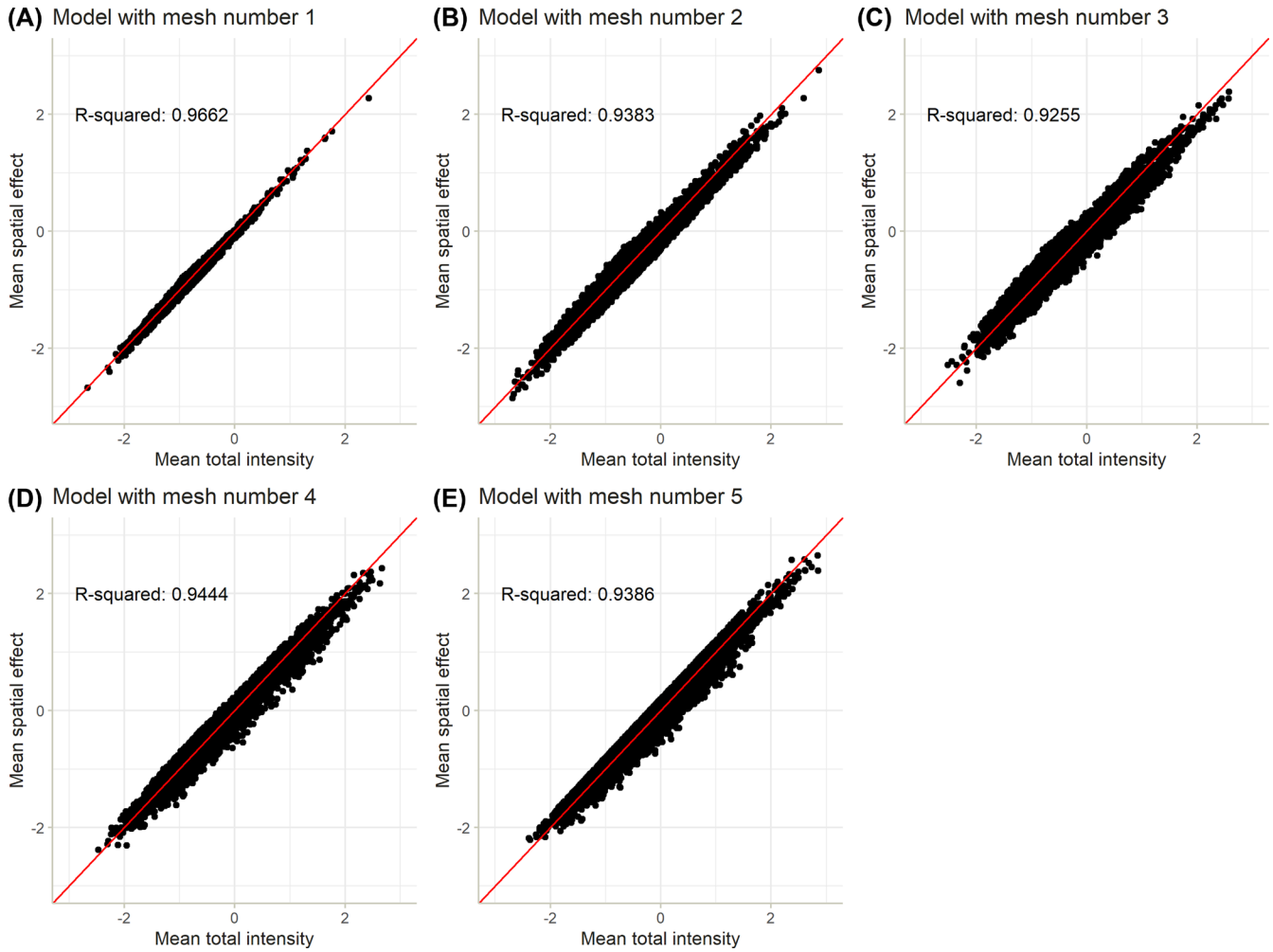

Figure 5. The correlation (R^2) between the total mean intensity and the intensity at a location as a function of the spatial effect. The red line indicates a slope of 1.

INLA–SPDE approach. It is commonly assumed that a finer mesh will lead to more accurate results with the only trade-off being computational cost (Blangiardo and Cameletti 2015). Yet, we found that the model with the finest mesh perfectly reproduced the spatial patterns found in our observations, thus was potentially overfitting. We demonstrate that spatial predictions became broader and less detailed with increased mesh coarseness. While these results indicate that coarser mesh density affects the level of accuracy in the predictions of spatial intensity, they also show that care must be taken to avoid overfitting by using a mesh that is too fine. These patterns are potentially surprising for those outside of the statistical literature, and something they should be aware of when using an INLA–SPDE approach to model species distributions.

We also found that the spatial effect became visually smoother with decreased mesh density. This may be an issue in a case like the one presented in this study, where the spatial effect accounts for most of the unexplained variation in the model, and could therefore have large impacts on inferences (Hodges and Reich 2010). Our results also revealed large differences between one another for the posterior fixed effects. A study modelling the distribution of waterfowl (Adde et al. 2021) using the same approach reported that mesh density had little influence on model estimates. However, close inspection of their models reveals that the effects of temperature were consistently closer to zero in models with finer meshes, which is consistent with the pattern we observe when moving from mesh number 3 to mesh number 1. They included an observational covariate to account for sampling bias, which our models did not have. However, we did run our models with a second spatial effect to attempt to account for sampling bias in the PO dataset, which did not change the overall pattern of results presented here (Supporting information). Adde et al. (2021) also fixed their PC priors, which we have also shown to make little difference to the results (Supporting information). Thus, methodological differences cannot explain why the effects of mesh density are so pervasive in our study.

One explanation for our results is that the scale of the spatial effect competes with the scale at which the covariates operate (Paciorek 2010). If the spatial effect is allowed

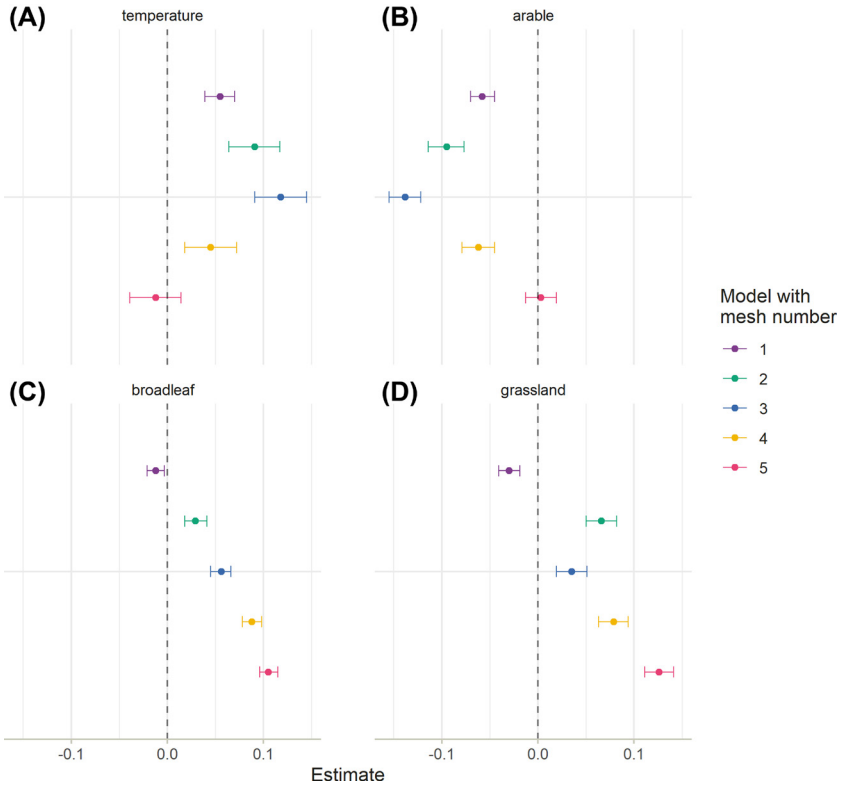

Figure 6. Posterior estimates of the environmental covariates: mean annual temperature (A), percentage cover arable land (B), broadleaf woodland (C), and improved grassland (D) for the five different models (Fig. 3, Table 1). Points indicate the mean of the different models, lines indicate the 95% credible intervals.

to operate at a finer scale than that of the covariates, it can create a situation in which the spatial effect explains all variation in the data, leading to over-fitting and under-estimation of the covariate effects (Illian et al. 2012; Illian and Burslem 2017). This could explain why the parameter estimates for temperature, which appears to be a limiting factor in the macro-scale distribution of *E. serotinus* (Fig. 1), increased from the finest (mesh number 1) to intermediate (mesh number 3) spatial effect (Fig. 6), but not why the estimates were lower for the two coarsest meshes (numbers 4 and 5). Estimates for arable land, which has broad spatial gradients in Britain (Fig. 2), showed a similar pattern. The remaining covariates – broadleaf woodland and grassland – vary at fine spatial scales, and determine the distribution of bats within landscapes, i.e. at smaller scales: parameter estimates for these variables increased with mesh coarseness. Thus, the relationship between the scale of the spatial effect and that of the covariates is not straightforward. Sørbye et al. (2019) also acknowledge the problems that arise from spatial processes operating at various spatial scales and demonstrate the use of PC priors to address these. However, they do not take the mesh-based approach needed for an INLA–SPDE model. In addition, they analyse data from a dataset that is spatially limited and where all species locations are known. In contrast, most ecological datasets, especially those used to fit SDMs and IDMs, are heterogeneous, incomplete, and often observed at a large scale. Future work is therefore required to better understand the interaction between PC priors and mesh parameterisation, especially as a way to deal with spatial confounding.

While it was not the aim of this study to establish which mesh parameterisation would result in the 'best' model in terms of model fit and predictive accuracy, the conclusions drawn from the results could have been strengthened if models had been validated formally. One approach for validating spatial data would be block cross-validation, where data are divided strategically rather than randomly into spatial, environmental, or temporal units ('blocks') (Roberts et al. 2017, Valavi et al. 2018). A newly released version of the 'PointedSDMs' R package (www.r-project.org) used in this study also includes a function to apply block cross-validation for IDMs (Morera-Pujol et al. 2022, Mostert and O'Hara 2022), which makes it easy and straightforward for future studies to validate models as standard. In addition, future work could also focus on conducting simulation studies to further explore the generalisability of the findings presented here.

Our results do raise questions about the degree to which INLA is a useful tool for modelling species distributions, especially using integrated models. In the absence of clearer guidance about the issues raised here, we recommend that modellers should present results from multiple meshes as a matter of course. Adopting this practice would have two benefits. First, it would recognise explicitly that the mesh is an important variable in the modelling process, rather than something that is

external, fixed, and already optimised. Second, it would generate a body of evidence about whether the phenomena we report are pervasive, or restricted to datasets with specific properties.

Point process models provide an intuitive framework to implement IDMs but some uncertainties remain, specifically surrounding the spatial effect, that cast doubt on inferences made from these models. Here, we have shown that mesh density affects both spatial predictions and the posterior estimates of the fixed effects. The parameterisation of the mesh is conceptually straightforward but requires the user to estimate the range; that is, the radius around an observation at which autocorrelation nears zero, for the problem at hand. Depending on the study species and the factors driving spatial autocorrelation, the potential values one might consider could range widely. We conclude that for those interested in the description of spatial patterns, the greatest problem may be overfitting from a mesh that is too fine. This could have knock-on effects for conservation measures, for example when trying to consider protection measures for important areas of the species' distribution. For those interested in the posterior covariate estimates, for example for climate change predictions, even greater care must be taken when parameterising the mesh. In particular, users should pay attention to the scale at which the spatial effect and the covariates are set to operate.

Acknowledgements – We thank Susan Jarvis, Dina Sadykova, Lia Gilmour, and Kit Stoner for valuable comments on previous versions of the manuscript. The National Bat Monitoring Programme (NBMP) is run by Bat Conservation Trust, in partnership with the Joint Nature Conservation Committee, and supported and steered by Natural England, Natural Resources Wales, Northern Ireland Environment Agency, and Scottish Natural Heritage. The NBMP is indebted to all observers who contribute data to the programme. *Funding* – We acknowledge financial support from NERC (PhD studentship NE/P010539/1 to LID).

Author contributions

Lea I. Dambly: Conceptualization (equal); Investigation (lead); Methodology-Supporting, Writing – original draft (lead); Writing – review and editing (equal). **Nick J. B. Isaac**: Conceptualization (equal); Funding acquisition (equal); Investigation (equal); Supervision (lead); Writing – original draft (equal); Writing – review and editing (equal). **Kate E. Jones**: Funding acquisition (equal); Supervision (equal); Writing – original draft (equal); Writing – review and editing (equal). **Katherine L. Boughey**: Funding acquisition (equal); Supervision (equal); Writing – original draft (equal). **Robert B. O'Hara**: Conceptualization (equal); Investigation (equal); Methodology (lead); Writing – original draft (equal); Writing – review and editing (equal).

Transparent peer review

The peer review history for this article is available at https://publons.com/publon/10.1111/ecog.06391.

Data availability statement

Code is available from the Github Digital Repository: https://github.com/LeaDambly/IM_serotine, and data are available from the Dryad Digital Repository: https://doi.org/10.5061/dryad.zgmsbcch5 (Dambly et al. 2023).

Supporting information

The Supporting information associated with this article is available with the online version.

References

Adde, A., Casabona i Amat, C., Mazerolle, M. J., Darveau, M., Cumming, S. G. and O'Hara, R. B. 2021. Integrated modeling of waterfowl distribution in western Canada using aerial survey and citizen science (eBird) data. – Ecosphere 12: e03790.

August, T., Harvey, M., Lightfoot, P., Kilbey, D., Papadopoulos, T. and Jepson, P. 2015. Emerging technologies for biological recording: emerging technologies for biological recording. – Biol. J. Linn. Soc. 115: 731–749.

Bakka, H. 2017. Mesh creation including coastlines. – https://haakonbakkagit.github.io/btopic104.html.

Bakka, H. 2018. A simple spatial model: simulation-inference. – https://haakonbakkagit.github.io/btopic122.html.

Barlow, K. E., Briggs, P. A., Haysom, K. A., Hutson, A. M., Lechiara, N. L., Racey, P. A., Walsh, A. L. and Langton, S. D. 2015. Citizen science reveals trends in bat populations: the National Bat Monitoring Programme in Great Britain. – Biol. Conserv. 182: 14–26.

Bayraktarov, E., Ehmke, G., O'Connor, J., Burns, E. L., Nguyen, H. A., McRae, L., Possingham, H. P. and Lindenmayer, D. B. 2019. Do big unstructured biodiversity data mean more knowledge? – Fron. Ecol. Evol. 6: 239.

Blangiardo, M. and Cameletti, M. 2015. Spatial and spatio-temporal Bayesian models with R-INLA. John Wiley and Sons, Inc.

Botts, E. A., Erasmus, B. F. N. and Alexander, G. J. 2011. Geographic sampling bias in the South African frog atlas project: implications for conservation planning. – Biodiver. Conserv. 20: 119–139.

Boughey, K. L., Lake, I. R., Haysom, K. A. and Dolman, P. M. 2011. Effects of landscape-scale broadleaved woodland configuration and extent on roost location for six bat species across the UK. – Biol. Conser. 144: 11.

Bowler, D. E., Nilsen, E. B., Bischof, R., O'Hara, R. B., Yu, T. T., Oo, T., Aung, M. and Linnell, J. D. C. 2019. Integrating data from different survey types for population monitoring of an endangered species: the case of the Eld's deer. – Sci. Rep. 9: 7766.

Catto, C. M. C., Hutson, A. M., Raccey, P. A. and Stephenson, P. J. 1996. Foraging behaviour and habitat use of the serotine bat (*Eptesicus serotinus*) in southern England. – J. Zool. 238: 623–633.

Chevalier, M., Broennimann, O., Cornuault, J. and Guisan, A. 2021. Data integration methods to account for spatial niche truncation effects in regional projections of species distribution. – Ecol. Appl. 31: e02427.

Dambly, L. I., Isaac, N. J. B., Jones, K. E., Boughey, K. L. and O'Hara, R. B. 2023. Data from: Integrated species distribution

models fitted in INLA are sensitive to mesh parameterisation. – Dryad Digital Repository, https://doi.org/10.5061/dryad.zgmsbcch5.
Dennis, R. L. H. and Thomas, C. D. 2000. Bias in butterfly distribution maps: the influence of hot spots and recorder's home range. – J. Insect Conserv. 4: 5.
Dietz, C., Helversen, O. von, Nill, D. and Lina, P. H. C. 2009. Serotine bat. – In: Dietz, C., Helversen, O. von and Nill, D. (eds), Bats of Britain, Europe and Northwest Africa. A & C Black, p. 400.
Dorazio, R. M. 2014. Accounting for imperfect detection and survey bias in statistical analysis of presence-only data. – Global Ecol. Biogeogr. 23: 1472–1484.
Farr, M. T., Green, D. S., Holekamp, K. E. and Zipkin, E. F. 2021. Integrating distance sampling and presence-only data to estimate species abundance. – Ecology 102: e03204.
Fithian, W., Elith, J., Hastie, T. and Keith, D. A. 2015. Bias correction in species distribution models: pooling survey and collection data for multiple species. – Methods Ecol. Evol. 15: 424–438.
Fletcher, R. J., Hefley, T. J., Robertson, E. P., Zuckerberg, B., Mccleery, R. A. and Dorazio, R. M. 2019. A practical guide for combining data to model species distributions. – Ecology 100: 15.
Geldmann, J., Heilmann-Clausen, J., Holm, T. E., Levinsky, I., Markussen, B., Olsen, K., Rahbek, C. and Tøttrup, A. P. 2016. What determines spatial bias in citizen science? Exploring four recording schemes with different proficiency requirements. – Divers. Distrib. 22: 1139–1149.
Gibb, R., Browning, E., Glover-Kapfer, P. and Jones, K. E. 2019. Emerging opportunities and challenges for passive acoustics in ecological assessment and monitoring. – Methods Ecol. Evol. 10: 169–185.
Gilbert, N. A., Pease, B. S., Anhalt-Depies, C. M., Clare, J. D. J., Stenglein, J. L., Townsend, P. A., Van Deelen, T. R. and Zuckerberg, B. 2021. Integrating harvest and camera trap data in species distribution models. – Biol. Conserv. 258: 109147.
Guillera-Arroita, G. 2016. Modelling of species distributions, range dynamics and communities under imperfect detection: advances, challenges and opportunities. – Ecography 40: 281–295.
Hampton, S. E., Strasser, C. A., Tewksbury, J. J., Gram, W. K., Budden, A. E., Batcheller, A. L., Duke, C. S. and Porter, J. H. 2013. Big data and the future of ecology. – Front. Ecol. Environ. 11: 156–162.
Held, L., Schrödle, B. and Rue, H. 2010. Posterior and cross-validatory predictive checks: a comparison of MCMC and INLA. – In: Kneib, T. and Tutz, G. (eds), Statistical modelling and regression structures. Physica-Verlag HD, pp. 91–110.
Hodges, J. S. and Reich, B. J. 2010. Adding spatially-correlated errors can mess up the fixed effect you love. – Amer. Statist. 64: 325–334.
Hutterer, R. (ed.) 2005. Bat migrations in Europe: a review of banding data and literature. – Federal Agency for Nature Conservation.
Illian, J. B., Sørbye, S. H. and Rue, H. 2012. A toolbox for fitting complex spatial point process models using integrated nested Laplace approximation (INLA). – Ann. Appl. Stat. 6: 32.
Illian, J. B., Martino, S., Sørbye, S. H. and Gallego-Ferna, J. B. 2013. Fitting complex ecological point process models with integrated nested Laplace approximation. – Methods Ecol. Evol. 11: 305–315.
Illian, J. B. and Burslem, D. F. R. P. 2017. Improving the usability of spatial point process methodology: an interdisciplinary dialogue between statistics and ecology. – AStA Adv. Stat. Anal. 101: 495–520.
Isaac, N. J. B., Jarzyna, M. A., Keil, P., Dambly, L. I., Boersch-Supan, P. H., Browning, E., Freeman, S. N., Golding, N., Guillera-Arroita, G., Henrys, P. A., Jarvis, S., Lahoz-Monfort, J., Pagel, J., Pescott, O. L., Schmucki, R., Simmonds, E. G. and O'Hara, R. B. 2020. Data integration for large-scale models of species distributions. – Trends Ecol. Evol. 35: 56–67.
Johnston, A., Matechou, E. and Dennis, E. B. 2022. Outstanding challenges and future directions for biodiversity monitoring using citizen science data. – Methods Ecol. Evol. 14: 103–116.
Kéry, M. and Royle, J. A. 2016. Applied hierarchical modeling in ecology: analysis of distribution, abundance and species richness in R and BUGS. – Elsevier/AP.
Koshkina, V., Wang, Y., Gordon, A., Dorazio, R. M., White, M. and Stone, L. 2017. Integrated species distribution models: combining presence-background data and site-occupancy data with imperfect detection. – Methods Ecol. Evol. 8: 420–430.
Krainski, E. T. (ed.) 2019. Advanced spatial modeling with stochastic partial differential equations using R and INLA. – CRC Press, Taylor & Francis Group.
Lindgren, F. and Rue, H. 2015. Bayesian spatial modelling with R-INLA. – J. Stat. Softw. 63: 1–25.
Lindgren, F., Rue, H. and Lindström, J. 2011. An explicit link between Gaussian fields and Gaussian Markov random fields: the stochastic partial differential equation approach. – J. R. Stat. Soc., B Stat. Methodol. 73: 423–498.
Mair, L. and Ruete, A. 2016. Explaining spatial variation in the recording effort of citizen science data across multiple taxa. – PLoS One 11: e0147796.
Mielke, K. P., Claassen, T., Busana, M., Heskes, T., Huijbregts, M. A. J., Koffijberg, K. and Schipper, A. M. 2020. Disentangling drivers of spatial autocorrelation in species distribution models. – Ecography 43: 1741–1751.
Miller, D. A. W., Pacifici, K., Sanderlin, J. S. and Reich, B. J. 2019. The recent past and promising future for data integration methods to estimate species' distributions. – Methods Ecol. Evol. 10: 16.
Miller, D. L., Glennie, R. and Seaton, A. E. 2020. Understanding the stochastic partial differential equation approach to smoothing. – J. Agric. Biol. Environ. Stat. 25: 1–16.
Møller, J., Syversveen, A. R. and Waagepetersen, R. P. 1998. Log Gaussian Cox processes. – Scand. J. Stat. 25: 451–482.
Morera-Pujol, V., Mostert, P. S., Murphy, K. J., Burkitt, T., Coad, B., McMahon, B. J., Nieuwenhuis, M., Morelle, K., Ward, A. I. and Ciuti, S. 2022. Bayesian species distribution models integrate presence-only and presence–absence data to predict deer distribution and relative abundance. – Ecography 2023: e06451.
Mostert, P. S. and O'Hara, R. B. 2022. PointedSDMs – an R package to help facilitate the construction of integrated species distribution models. – bioRxiv 2022.10.06.511075.
Pacifici, K., Reich, B. J., Miller, D. A. W., Gardner, B., Stauffer, G., Singh, S., McKerrow, A. and Collazo, J. A. 2017. Integrating multiple data sources in species distribution modeling: a framework for data fusion. – Ecology 98: 840–850.
Paciorek, C. J. 2010. The importance of scale for spatial-confounding bias and precision of spatial regression estimators. – Stat. Sci. 25: 107–125.
Peel, S. L., Hill, N. A., Foster, S. D., Wotherspoon, S. J., Ghiglione, C. and Schiaparelli, S. 2019. Reliable species distributions are

obtainable with sparse, patchy and biased data by leveraging over species and data types. – Methods Ecol. Evol. 10: 1002–1014.
Renner, I. W., Elith, J., Baddeley, A., Fithian, W., Hastie, T., Phillips, S. J., Popovic, G. and Warton, D. I. 2015. Point process models for presence-only analysis. – Methods Ecol. Evol. 6: 366–379.
Roberts, D. R., Bahn, V., Ciuti, S., Boyce, M. S., Elith, J., Guillera-Arroita, G., Hauenstein, S., Lahoz-Monfort, J. J., Schröder, B., Thuiller, W., Warton, D. I., Wintle, B. A., Hartig, F. and Dormann, C. F. 2017. Cross-validation strategies for data with temporal, spatial, hierarchical, or phylogenetic structure. – Ecography 40: 913–929.
Robinson, E. L., Blyth, E., Clark, D. B., Comyn-Platt, E., Finch, J. and Rudd, A. C. 2017. – Climate hydrology and ecology research support system meteorology dataset for Great Britain (1961–2015) [CHESS-met] v1.2, https://catalogue.ceh.ac.uk/documents/b745e7b1-626c-4ccc-ac27-56582e77b900 doi: https://doi.org/10.5285/b745e7b1-626c-4ccc-ac27-56582e77b900.
Robinson, M. F. and Stebbings, R. E. 1997. Home range and habitat use by the serotine bat, *Eptesicus serotinus*, in England. – J. Zool. 243: 117–136.
Rowland, C. S., Morton, R. D., Carrasco, L., McShane, G., O'Neil, A. W. and Wood, C. M. 2017. – Land cover map 2015 (1 km percentage aggregate class, GB), https://catalogue.ceh.ac.uk/documents/b745e7b1-626c-4ccc-ac27-56582e77b900 doi: https://doi.org/10.5285/b745e7b1-626c-4ccc-ac27-56582e77b900.
Rue, H., Martino, S. and Chopin, N. 2009. Approximate Bayesian inference for latent Gaussian models by using integrated nested Laplace approximations. – J. R. Stat. Soc. Ser. B Stat. Methodol. 71: 319–392.
Simmonds, E. G., Jarvis, S. G., Henrys, P. A., Isaac, N. J. B. and O'Hara, R. B. 2020. Is more data always better? A simulation study of benefits and limitations of integrated distribution models. – Ecography 43: 10.
Simpson, D., Illian, J. B., Lindgren, F., Sørbye, S. H. and Rue, H. 2016. Going off grid: computationally efficient inference for log-Gaussian Cox processes. – Biometrika 103: 49–70.
Simpson, D., Rue, H., Riebler, A., Martins, T. G. and Sørbye, S. H. 2017. Penalising model component complexity: a principled, practical approach to constructing priors. – Stat. Sci. 32: 1–28.
Sørbye, S. H., Illian, J. B., Simpson, D. P., Burslem, D. and Rue, H. 2019. Careful prior specification avoids incautious inference for log-Gaussian Cox point processes. – J. R. Stat. Soc., C Appl. Stat. 68: 543–564.
Strebel, N., Kéry, M., Guélat, J. and Sattler, T. 2022. Spatiotemporal modelling of abundance from multiple data sources in an integrated spatial distribution model. – J. Biogeogr. 49: 563–575.
Tink, M., Burnside, N. G. and Waite, S. 2014. A spatial analysis of serotine bat (*Eptesicus serotinus*) roost location and landscape structure: a case study in Sussex, UK. – Int. J. Biodivers. 10: 1–9.
Valavi, R., Elith, J., Lahoz-Monfort, J. J. and Guillera-Arroita, G. 2018. BLOCK CV : an R package for generating spatially or environmentally separated folds for k-fold cross-validation of species distribution models.. – Methods Ecol. Evol. 10: 225–232.
Zipkin, E. F., Inouye, B. D. and Beissinger, S. R. 2019. Innovations in data integration for modeling populations. – Ecology 100: e02713.